



OPEN An incentive-aware federated bargaining approach for client selection in decentralized federated learning for IoT smart homes

Jai Vinita L

Federated Learning (FL) has emerged as a promising solution for privacy-preserving model training across distributed IoT devices. Despite its advantages, FL faces challenges such as inefficient client selection, data heterogeneity, security vulnerabilities, and exposure to Man-in-the-Middle (MITM) attacks. To address these issues, the Incentive-Aware Federated Bargaining (IAFB) framework is proposed, integrating Nash Bargaining for optimal client selection, Shapley-value-based incentives for fair reward distribution, and decentralized peer-to-peer (P2P) aggregation to eliminate single points of failure. To enhance security, IAFB employs AES-GCM encryption, ensuring data confidentiality, authenticity, and integrity during transmission, effectively mitigating MITM attacks. Experimental results demonstrate that IAFB improves participation fairness by 28%, boosts model accuracy by 6.5%, and reduces convergence time by 35% compared to FedAvg. Additionally, IAFB reduces communication overhead by 39.5% and enhances resilience against adversarial threats, making it highly suitable for secure and scalable FL deployment in resource-constrained IoT environments.

Keywords Federated learning, Client selection, Nash bargaining solution, Incentive mechanism, IoT smart homes

The rapid proliferation of IoT smart home ecosystems, where interconnected devices generate sensitive user data, necessitates secure and efficient collaborative learning solutions that preserve privacy while enabling intelligent applications^{1,2}. Federated Learning (FL) offers a promising approach by allowing distributed devices to collaboratively train a global model without sharing raw data, thereby reducing the risk of data breaches and enhancing user privacy³. However, deploying FL in heterogeneous and resource-constrained IoT environments is hindered by challenges such as inefficient client selection, data heterogeneity, security vulnerabilities, and insufficient incentives for participation⁴.

Traditional FL frameworks like FedAvg¹ and FedSGD² rely on random client selection, which overlooks variations in device capabilities, data quality, and energy constraints, leading to suboptimal training outcomes⁵. Security threats, such as model poisoning and Man-in-the-Middle (MITM) attacks, exploit vulnerabilities in model update exchanges, compromising FL reliability^{6,7}. Moreover, non-independent and identically distributed (non-IID) data across IoT devices causes biased models and reduced accuracy³. Existing solutions like FedProx⁸ and MOON⁹ address data heterogeneity but fail to optimize client selection or incentivize sustained participation. Additionally, the lack of fair incentives discourages devices from contributing, as local training consumes significant resources¹⁰.

To address these challenges, we propose the Incentive-Aware Federated Bargaining (IAFB) framework, designed to enable secure, fair, and efficient FL in IoT smart home environments. IAFB employs Nash Bargaining to optimize client selection, balancing device utility (e.g., energy, data quality) with aggregator goals (e.g., model accuracy), ensuring fair participation. A Shapley-value-based incentive mechanism rewards clients proportionally to their contributions, mitigating free-riding and encouraging sustained engagement¹⁰. To bolster security, IAFB integrates AES-GCM encryption to protect model updates against MITM attacks, ensuring confidentiality, authenticity, and integrity⁷. Additionally, a decentralized peer-to-peer (P2P) aggregation mechanism eliminates

School of Computing Science and Engineering, Vellore Institute of Technology, Chennai Campus, Chennai, India.
email: jaivinita.l@vit.ac.in

single points of failure, enhancing resilience against adversarial threats⁶. Extensive experiments demonstrate that IAFB achieves a 28% improvement in participation fairness, a 6.5% increase in model accuracy, a 35% reduction in convergence time, and a 39.5% decrease in communication overhead compared to FedAvg¹.

The primary motivation of this work is to facilitate scalable, privacy-preserving intelligence in IoT smart homes, fostering user trust through robust security and equitable participation. IAFB addresses critical FL challenges, making it a practical solution for real-world IoT applications.

The contributions of this work include the following.

- A Nash bargaining-based client selection mechanism for fair and optimal participation¹
- A Shapley-value-based incentive system to ensure equitable rewards¹⁰
- A decentralized P2P aggregation approach for enhanced security⁶
- AES-GCM encryption to mitigate MITM attacks⁷
- Comprehensive experimental validation demonstrating significant performance improvements.

The remainder of this paper is structured as follows: “Related work” reviews related work, “Proposed system” details the IAFB framework, “Performance evaluation” presents experimental evaluations, and “Conclusion” concludes the paper.

2. Related work

Federated Learning (FL) enables privacy-preserving model training across distributed IoT devices, but its deployment in smart home environments faces challenges in client selection, data heterogeneity, security, and incentives¹. This section analyzes prior work on FL frameworks, client selection, incentive mechanisms, Nash Bargaining, and security, highlighting their strengths and weaknesses to contextualize the research landscape. We incorporate recent top-venue articles^{11–15} for a comprehensive review, with the Incentive-Aware Federated Bargaining (IAFB) framework’s contributions discussed in Section 2.6.

2.1 Federated learning in IoT smart homes

FL supports privacy-preserving training in IoT smart homes by enabling local model updates on devices like sensors and thermostats^{1,2}. FedAvg¹ and FedSGD² use random client selection and weighted averaging, offering simplicity and scalability for large-scale IoT networks. However, their assumption of uniform client capabilities leads to biased models due to device heterogeneity and data imbalance⁵. FedProx⁸ introduces a proximal term to handle data heterogeneity, making it robust for diverse IoT datasets, but its increased computational complexity slows convergence and it lacks mechanisms for fairness or incentives. MOON⁹ employs model-contrastive learning to align local and global models, excelling in non-IID settings common in smart homes, but its absence of incentive mechanisms limits client participation. Zhang et al.¹⁴ enhance security with differential privacy, providing strong privacy guarantees, but their approach neglects incentives, reducing participation in resource-constrained environments.

2.2 Client selection strategies in federated learning

Effective client selection is critical for FL performance in heterogeneous IoT environments⁵. Random selection in FedAvg and FedSGD^{1,2} is computationally lightweight, enabling fast deployment, but ignores device heterogeneity, leading to suboptimal updates and model bias⁴. Resource-aware strategies¹⁶ prioritize computational power and bandwidth, improving efficiency for IoT devices, but often overlook data diversity, resulting in biased models. Liu et al.¹¹ use reinforcement learning to dynamically select clients based on data quality, enhancing model performance, but the approach requires extensive training and struggles with scalability in dynamic IoT settings.

2.3 Incentive mechanisms for federated learning

Sustaining client participation in FL requires equitable incentives, particularly for resource-constrained IoT devices¹⁰. Monetary reward systems^{10,17} are straightforward to implement, encouraging participation, but often ignore data quality, leading to cost inefficiencies and unfair rewards. Reputation-based systems¹⁰ promote engagement through trust scores but are vulnerable to manipulation by adversarial clients. Ma et al.¹² propose blockchain-based incentives, offering transparency and security, but their high computational overhead makes them impractical for IoT devices. Surveys like Tahir et al.¹⁸ note that existing mechanisms struggle with scalability and fairness in IoT contexts.

2.4 Nash bargaining for fair client selection

Game-theoretic models address client selection fairness in FL⁵. Contract theory¹⁰ and auction-based pricing¹⁷ optimize aggregator utility, enabling efficient resource allocation, but often prioritize aggregator benefits over client fairness, leading to imbalanced participation. Wang et al.¹⁵ apply game-theoretic fairness in cloud-based FL, achieving balanced utility distribution, but their approach’s high resource demands are unsuitable for IoT environments. Nash Bargaining^{5,16} provides a balanced framework for resource allocation, ensuring equitable participation, but prior implementations often lack integration with incentives or security mechanisms.

2.5 Security challenges and man-in-the-middle attacks in FL

FL’s localized training enhances privacy but remains vulnerable to model poisoning, backdoor attacks, and man-in-the-middle (MITM) attacks^{6,7}. Secure aggregation and homomorphic encryption¹⁹ offer robust security, protecting against data breaches, but their computational intensity is impractical for IoT devices. Fekri et al.¹³ emphasize differential privacy and secure multi-party computation in healthcare FL, providing strong privacy

but reducing model accuracy due to added noise. Zhang et al.¹⁴ combine differential privacy with secure aggregation, balancing privacy and efficiency, but their approach is less effective against MITM attacks.

2.6 Summary and research gaps

Despite advancements in FL, critical gaps remain:

- Random selection methods^{1,2} are simple but biased due to heterogeneity and data imbalance.
- FedProx⁸ is robust to heterogeneity but computationally heavy, lacking fairness mechanisms.
- MOON⁹ excels in non-IID settings but lacks incentives, limiting participation.
- Liu et al.¹¹ improve selection but require high training costs, hindering scalability.
- Ma et al.¹² provide transparent incentives but incur high overhead, unsuitable for IoT.
- Fekri et al.¹³ ensure privacy but sacrifice accuracy.
- Centralized architectures⁶ are vulnerable to single points of failure.

The IAFB framework addresses these gaps through Nash Bargaining for fair client selection, Shapley-value-based incentives for equitable rewards, decentralized P2P aggregation for resilience, and AES-GCM encryption for efficient security, providing a holistic solution for IoT smart homes, as detailed in “Proposed system” and validated in “Performance evaluation”.

3. Proposed system

Federated Learning in IoT smart homes presents challenges related to inefficient client selection, data heterogeneity, security threats, and lack of incentive mechanisms. The proposed Incentive-Aware Federated Bargaining (IAFB) framework addresses these limitations by eliminating centralized servers and employing a decentralized peer-to-peer aggregation mechanism. The framework integrates Nash Bargaining-based client selection, Shapley-value-based incentive ranking, and decentralized model aggregation, ensuring fair participation, robust security, and optimal resource utilization.

The proposed framework operates in a fully distributed manner, where multiple aggregators coordinate model training and merging without relying on a single central server. Unlike traditional learning methods that assume uniform participation, the proposed framework dynamically selects clients based on their utility scores, considering computational capacity, data quality, and energy availability. The incentive mechanism further ensures that participating clients are fairly rewarded based on their contributions to the global model, discouraging free-riding behavior and malicious updates.

3.1 System architecture

The IAFB architecture, illustrated in Fig. 1, consists of three layers designed to achieve decentralized, efficient, and secure FL:

- IoT clients: smart home devices (e.g., cameras, thermostats) perform local training on private data, reducing communication by sending only model updates to edge aggregators.
- Federated edge aggregation: edge servers receive encrypted updates, perform local aggregation to minimize bandwidth usage, and filter anomalies to ensure model integrity, serving as an intermediate step to offload processing from peer aggregators.
- Peer aggregators: a decentralized network of aggregators merges edge-aggregated models, with a rotating leader selected via round-robin to coordinate global model computation using weighted averaging. The rotating leader ensures fault tolerance without persistent central control, aligning with decentralization.

A full training round operates as follows:

1. Client selection: IoT clients are selected via Nash Bargaining (“Client selection strategies in federated learning”) based on utility scores, determining which devices participate.
2. Local training: selected clients train local models on their private data.
3. Secure transmission: clients encrypt updates using AES-GCM (Sect. ??) and send them to edge aggregators.
4. Edge aggregation: edge servers aggregate encrypted updates locally, filtering anomalies, and forward the results to peer aggregators.
5. Peer-to-peer aggregation: peer aggregators, coordinated by a rotating leader, merge edge-aggregated models into a global model using weighted averaging (Section 3.4).
6. Incentive calculation: Shapley-value incentives are computed to reward clients (“Incentive mechanisms for federated learning”).
7. Model distribution: the leader distributes the global model to peer aggregators, which relay it to edge servers and back to clients for the next round.

This workflow ensures a seamless process from client selection to model distribution. The process begins with client selection (“Client selection strategies in federated learning”), integrates incentives (“Incentive mechanisms for federated learning”), and secures updates (Sect. ??).

3.2 Client selection with Nash bargaining

IAFB employs Nash Bargaining to select clients, optimizing participation by balancing computational capacity, data quality, and energy constraints. For instance, in a smart home, a thermostat with high-quality temperature data might be prioritized over a low-energy motion sensor, reflecting resource allocation principles seen in IIoT, ensuring efficient use of energy-constrained devices. The framework models client selection as a Nash

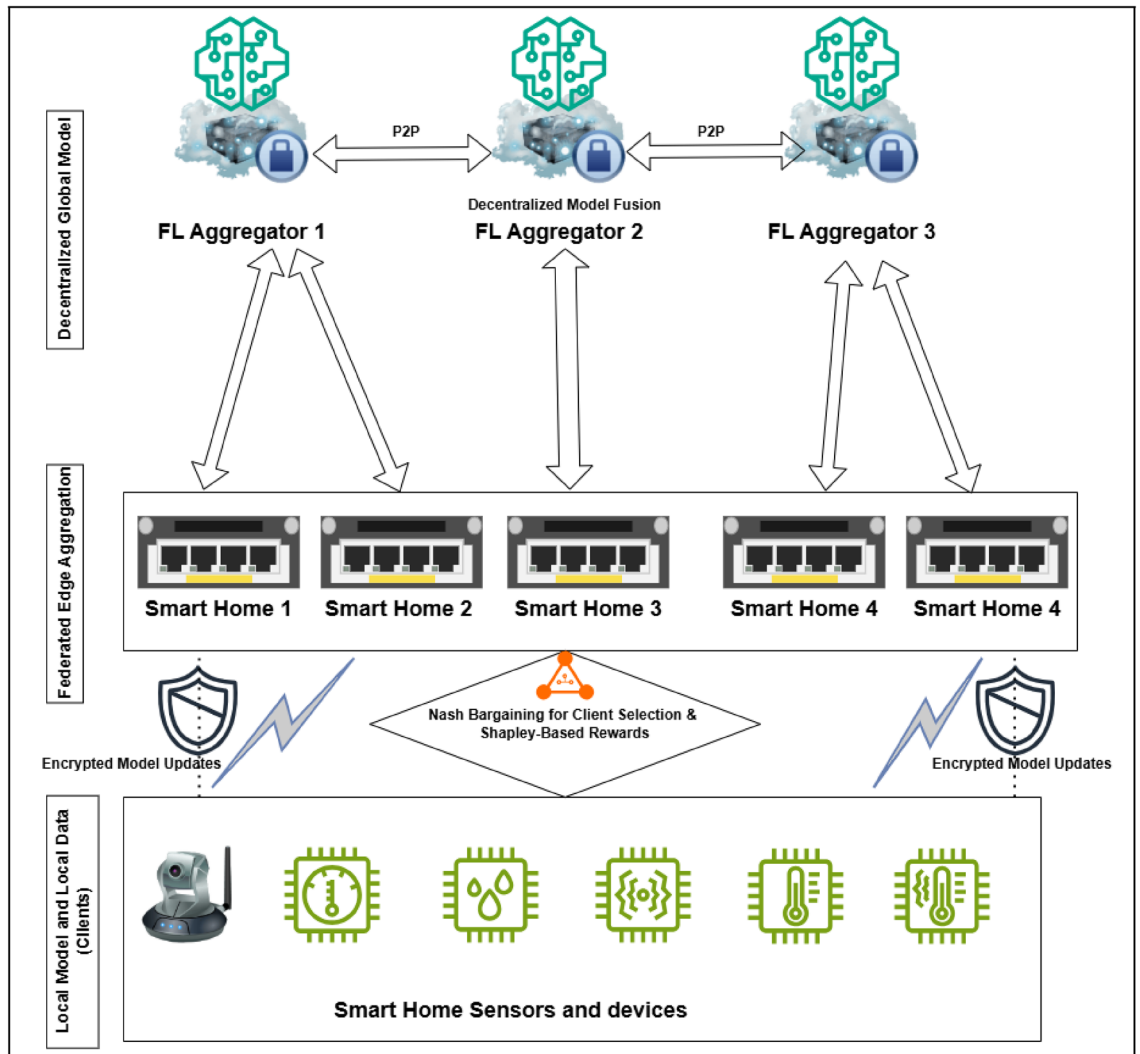


Fig. 1. Incentive-aware federated bargaining system architecture (arrows showing data flow from IoT clients to edge aggregators to peer aggregators, and labels for rotating leader coordination).

Bargaining problem, where each client negotiates participation based on its utility function. The utility function U_i for each client c_i is defined as:

$$U_i = \alpha D_q + \beta C_p - \gamma E_c - \delta P_r,$$

where D_q represents the data quality of the client, C_p denotes the computational power, E_c accounts for energy constraints, P_r measures the risk of privacy.

The Nash Bargaining process maximizes the joint utility function across all selected clients:

$$U^* = \arg \max \prod_{i=1}^n (U_i - U_{min}),$$

where U_{min} is the minimum acceptable utility threshold. Clients satisfying $U_i \geq U_{min}$ are selected for the training round.

This approach ensures fair and efficient client participation. Selected clients train local models, which are rewarded via incentives (“Incentive mechanisms for federated learning”) and secured by encryption (Sect. ??).

3.3 Shapley-value-based incentive mechanism

To encourage sustained participation, IAFB assigns rewards \mathcal{R}_i based on Shapley values ϕ_i , quantifying each client’s marginal contribution with an adaptive adjustment. For example, in a smart home, a camera detecting unique motion patterns for security might receive higher rewards, mirroring collaborative learning in smart devices, justifying its use to incentivize valuable data contributions in energy-efficient settings. The Shapley value for each client is calculated as follows:

$$\phi_i = W_{prev} \cdot \sum_{S \subseteq C \setminus \{i\}} \frac{|S|!(|C| - |S| - 1)!}{|C|!} (V(S \cup \{i\}) - V(S)),$$

where S represents a subset of clients, $V(S)$ is the validation accuracy achieved using the subset S , C is the set of all clients, W_{prev} is a performance weight derived from the client's contribution in the previous round, reduced for poor performance or malicious behavior detected via anomaly filtering in edge aggregation.

The reduction of W_{prev} is determined as follows: for poor performance, if the marginal contribution $V(S \cup \{i\}) - V(S)$ falls below a threshold (e.g., mean contribution minus 2 standard deviations), $W_{prev} = \max(0, 1 - \alpha \cdot (1 - V_{prev}/V_{mean}))$, where α is a penalty factor (e.g., 0.5), V_{prev} is the client's prior round accuracy contribution, and V_{mean} is the average contribution. For malicious behavior, anomaly filtering in edge aggregation measures the Euclidean distance of the client's update W_i from the mean update; if this distance exceeds a threshold (e.g., mean + 2 standard deviations), $W_{prev} = 1 - \beta \cdot M_{flag}$, where β is a severity factor (e.g., 0.7) and M_{flag} is 1 for flagged anomalies, 0 otherwise. This ensures W_{prev} ranges from 0 to 1, penalizing underperformers or malicious clients.

The total reward pool is distributed proportionally among participating clients based on their Shapley values:

$$\mathcal{R}_i = \frac{\phi_i}{\sum_{j \in C} \phi_j} \cdot \mathcal{R}_{total}.$$

This adaptive mechanism reinforces the fairness of Nash Bargaining selection, supporting the secure aggregation process ("Client selection with Nash bargaining"), and ensures the system adjusts rewards dynamically based on prior round outcomes, impacting future selection.

3.4 AES-GCM encryption for secure transmission

AES-GCM provides confidentiality, authenticity, and integrity. Key exchange is performed using Diffie-Hellman (DH) during initial setup, enabling secure generation of symmetric keys K_{ci} between each client c_i and the corresponding edge aggregator. DH's lightweight nature suits IoT constraints, allowing secure key establishment over insecure channels without prior secrets. Key management involves secure distribution via Elliptic Curve Cryptography (ECC)-based channels and rotation of keys per training round to mitigate risks of key compromise. ECC's efficiency (smaller key sizes for equivalent security) supports limited resource IoT devices, ensuring robust distribution and rotation across the decentralized network. In multi-party settings, each client c_i uses a unique K_{ci} , allowing edge aggregators to aggregate encrypted updates without decryption using non-interactive zero-knowledge proofs for integrity verification, while peer aggregators decrypt only during global computation to ensure security across multiple parties.

The encryption process is defined as follows:

$$E_i = \text{Encrypt}(W_i, K_{ci}) \quad (1)$$

where W_i is the local model update, K_{ci} is the symmetric encryption key assigned to client c_i , and E_i is the encrypted model update.

During decryption, the MAC tag verifies data integrity:

$$W_i = \text{Decrypt}(E_i, K_{ci}) \quad (2)$$

This ensures any tampered data is identified and discarded. The encrypted updates are transmitted securely to the Federated Edge Aggregation layer for preliminary aggregation before being forwarded to the final aggregation stage.

3.5 Decentralised peer to peer model aggregation

The final global model is derived through a weighted averaging mechanism that integrates contributions from both the Federated Edge Aggregation layer and the decentralized peer-to-peer aggregation network. The updated model aggregation strategy is as follows:

$$W_{global} = \sum_{j=1}^m \frac{n_j}{N} W_j,$$

where W_j is the aggregated model from each Federated Edge Aggregator A_j , n_j is the number of clients associated with aggregator A_j , N is the total number of clients.

The aggregation process for each Federated Edge Aggregator's model, W_j , is defined as follows:

$$W_j = \sum_{i=1}^{n_j} \frac{|D_i|}{\sum_{k=1}^{n_j} |D_k|} W_i$$

where W_i is the local model update from client c_i , D_i is the dataset size of client c_i , n_j is the number of clients contributing to aggregator A_j .

This refined model aggregation ensures that client contributions are weighted appropriately, improving robustness against adversarial attacks and enhancing overall model accuracy.

The algorithm of the IAFB framework is divided into two phases: Client Selection and Local Training 1, followed by Model Aggregation and Incentive Calculation 2. The design optimizes computational efficiency while ensuring fairness, security, and robustness in IoT smart home environments. The structured design ensures improved participation fairness, robust security through AES-GCM, and minimized communication overhead using the leader-based P2P aggregation strategy. To ensure fairness and simplicity, a rotational selection method is used to choose the leader FL aggregator. This method rotates the leader role among all FL aggregators in a round-robin fashion, ensuring that each aggregator gets an equal opportunity to act as the leader. Multiple aggregations are necessary to optimize efficiency and consistency: the edge layer performs local aggregation to reduce communication overhead and filter anomalies, ensuring efficient processing at the device level, while the peer layer conducts global aggregation to achieve decentralized model consistency across the network.

```

1: Input: Set of IoT clients  $C = \{c_1, c_2, \dots, c_n\}$ , FL Aggregators  $A = \{A_1, A_2, \dots, A_m\}$ , global rounds  $T$ , reward pool  $R_{total}$ 
2: Output: Local Model Updates  $W_j$ 
3: for each global round  $t \in T$  do
4:   for each FL Aggregator  $A_j \in A$  in parallel do
5:     Client Selection using Nash Bargaining
6:     for each client  $c_i \in C_j$  do
7:       Compute Utility:  $U_i = \alpha D_q + \beta C_p - \gamma E_c - \delta P_r$ 
8:     end for
9:     Select clients satisfying  $U_i \geq U_{min}$ 
10:    Local Training and Secure Update Transmission
11:    for each selected client  $c_i$  do
12:      Train local model:  $W_i = \text{Train}(D_i, W_{global})$ 
13:      Encrypt update using AES-GCM:
           $E_i = \text{Encrypt}(W_i, K_{c_i})$ 
14:      Send  $(E_i, \text{MAC})$  to FL Aggregator  $A_j$ 
15:    end for
16:  end for
17: end for

```

Algorithm 1. IAFB: client selection and local training phase.

-
- 1: **for** each FL Aggregator A_j **do**
 - 2: **Local Aggregation at FL Aggregator**
 - 3: **for** each received update (E_i, MAC) **do**
 - 4: Verify integrity:
 - $W_i = \text{Decrypt}(E_i, K_{ci})$
 - 5: Aggregate model updates:
 - $$W_j = \sum_i \frac{|D_i|}{\sum_i |D_i|} W_i$$
 - 6: **end for**
 - 7: **end for**
 - 8: **Leader-Based Global Model Aggregation**
 - 9: Choose a Leader Aggregator A_L for global model computation
 - 10: Each FL Aggregator sends W_j to Leader Aggregator
 - 11: Compute final global model using weighted averaging:

$$W_{global} = \sum_{j=1}^m \frac{n_j}{N} W_j$$

- 12: **Shapley-Value-Based Incentive Calculation**

- 13: **for** each selected client c_i **do**
- 14: Compute Shapley value:

$$\phi_i = \sum_{S \subseteq C \setminus \{i\}} \frac{|S|!(|C| - |S| - 1)!}{|C|!} (V(S \cup \{i\}) - V(S))$$

- 15: Assign reward:

$$R_i = \frac{\phi_i}{\sum_{j \in C} \phi_j} \cdot R_{total}$$

- 16: **end for**
 - 17: **Model Distribution**
 - 18: Leader Aggregator A_L distributes W_{global} to all peer FL Aggregators A_j (where $j \neq L$)
 - 19: **for** each FL Aggregator A_j **do**
 - 20: Distribute W_{global} to the set of clients for the next communication round
 - 21: **end for**
-

Algorithm 2. IAFB: model aggregation and incentive calculation phase.

3.6 Complexity analysis

To evaluate the efficiency of the Incentive-Aware Federated Bargaining (IAFB) framework, we analyze the computational and communication complexity of its key components: Nash Bargaining-based client selection, local training, AES-GCM encryption, decentralized peer-to-peer (P2P) model aggregation, and Shapley-value-based incentive calculation.

- Nash bargaining-based client selection: the client selection process solves a Nash Bargaining problem to maximize the joint utility function across n clients. Computing the utility U_i for each client requires $O(1)$ time, as it involves a weighted sum of data quality, computational power, energy constraints, and privacy risk. The optimization $\arg \max \prod_{i=1}^n (U_i - U_{min})$ is approximated using a greedy algorithm, evaluating pairwise interactions, yielding a time complexity of $O(n^2)$. Space complexity is $O(n)$ for storing utility scores.
- Local training: each selected client trains a Long Short-Term Memory (LSTM) model on its local dataset D_i . For a dataset of size $|D_i|$ and model size m (number of parameters), training for E epochs with batch size B has a time complexity of $O(E \cdot |D_i| \cdot m)$. Space complexity is $O(m)$ for the model parameters and $O(B)$ for batch processing.

Component	Time complexity	Space complexity	Comm. complexity
Client selection	$O(n^2)$	$O(n)$	–
Local training	$O(E \cdot D_i \cdot m)$	$O(m + B)$	–
AES-GCM encryption	$O(m)$	$O(m)$	$O(m)$
Edge aggregation	$O(n_j \cdot m)$	$O(m)$	$O(n_j \cdot m)$
Global aggregation	$O(M \cdot m)$	$O(m)$	$O(M \cdot m)$
Incentive calculation	$O(n \cdot k \cdot m)$	$O(n)$	–

Table 1. Complexity analysis of IAFB components.

Component	Specification
CPU	Intel Core i7-11700K (3.6 GHz)
GPU	NVIDIA RTX 3090 (24 GB VRAM)
RAM	32 GB DDR4
Storage	1 TB SSD
Operating system	Ubuntu 20.04 LTS
Frameworks used	PyTorch 1.12, TensorFlow 2.10

Table 2. Hardware specifications for experimental setup.

Attribute	CASA smart home	MNIST
Number of clients	100	100
Number of features	15 (motion, temp., etc.)	784 (28 x 28 pixels)
Data type	Time-series	image
Data split	70% train, 15% val., 15% test	70% Train, 15% val., 15% test
Scaling method	Min-max normalization	Min-max normalization

Table 3. Dataset details.

- AES-GCM encryption: each client encrypts its model update W_i (size m) using AES-GCM with a 256-bit key. Encryption and decryption operations are linear in the data size, with time complexity $O(m)$. The space complexity is $O(m)$ for storing the encrypted update, initialization vector, and MAC tag.
- Decentralized P2P model aggregation: the Federated Edge Aggregation layer aggregates updates from n_j clients per aggregator A_j , weighted by dataset size, with time complexity $O(n_j \cdot m)$. For M aggregators, the leader-based global aggregation computes W_{global} by weighted averaging of M local models, with time complexity $O(M \cdot m)$. Communication complexity includes $O(n_j \cdot m)$ for client-to-edge transmission per aggregator and $O(M \cdot m)$ for aggregator-to-leader transmission. Space complexity is $O(m)$ per aggregator.
- Shapley-value-based incentive calculation: the Shapley value ϕ_i for each client quantifies its contribution to the global model. Exact computation has $O(2^n)$ time complexity, which is infeasible for large n . We use Monte Carlo sampling with k samples, reducing the time complexity to $O(n \cdot k \cdot m)$ for evaluating model accuracy on subsets. Space complexity is $O(n)$ for storing Shapley values.

Table 1 summarizes the complexity of each component.

This analysis demonstrates that IAFB is computationally efficient, with polynomial time complexity for client selection and aggregation, and optimized Shapley-value computation via sampling, making it suitable for resource-constrained IoT smart home environments.

4. Performance evaluation

4.1 Implementation details

The Incentive-Aware Federated Bargaining (IAFB) framework is evaluated using the CASA Smart Home dataset, comprising time-series IoT sensor data (e.g., motion, temperature, energy usage) from real-world smart home environments, and the MNIST dataset for image classification to validate generalizability. Both datasets are normalized using Min-Max scaling. Each smart home or MNIST client (100 clients) trains a Long Short-Term Memory (LSTM) model for CASA or a convolutional neural network (CNN) for MNIST using PyTorch, optimized with the Adam optimizer. Training occurs over 100 global rounds, with Nash Bargaining-based client selection, leader-based P2P aggregation, Shapley-value incentives, and AES-GCM encryption. The Federated Edge Aggregation layer filters suspicious updates, enhancing robustness and efficiency.

Hyperparameter	Value
Learning rate	0.001
Optimizer	Adam
Batch size	32
Epochs per round	10
Number of global rounds	100
Loss function	MSE (CASA), cross-entropy (MNIST)

Table 4. Training hyperparameters for IAFB framework.

Encryption parameter	Value
Encryption algorithm	AES-GCM
Key size	256-bit
Initialization vector (IV)	12 bytes
Tag size	16 bytes

Table 5. AES-GCM encryption configuration.

Device type	CPU	Memory	Energy capacity
Low-power sensor	ARM Cortex-M4	256 KB RAM	Limited (battery)
Smart thermostat	ARM Cortex-A7	512 MB RAM	Moderate (wall-powered)
High-performance hub	Intel Core i5	8 GB RAM	High (permanent power)
FL edge aggregator	ARM Cortex-A53	2 GB RAM	High (wall-powered)
FL aggregator	Intel Xeon	16 GB RAM	Very high (permanent power)

Table 6. Modeled IoT client, FL edge aggregator, and FL aggregator profiles.

Stage	Time (per round)	Memory usage (MB)
Client model training	1–2 mins	512
Federated edge aggregation	500 ms–2 s	128
Peer-to-peer model aggregation	1–5 s	256

Table 7. Training time and resource utilization.

Metric	FedAvg	FedProx	MOON	¹¹	¹²	¹³	IAFB
Participation rate (%)	62	71	75	80	78	73	89
Model accuracy (%)	78.5	82.3	84.7	85.5	83.2	79.2	91.2
Convergence time (rounds)	135	120	105	103	110	115	88
Security resilience	Low	Moderate	Moderate	Moderate	High	High	High
Comm. overhead (MB/round)	12.4	10.8	9.2	9.0	9.0	8.6	7.5
Acc. drop (attack) (%)	18.2	12.5	9.6	8.5	7.2	6.8	5.3
Client dropout rate (%)	21.5	14.3	10.1	9.0	8.5	9.5	4.2
Fairness (Gini coefficient)	0.42	0.31	0.25	0.26	0.29	0.30	0.18

Table 8. Performance comparison on CASA dataset. Significant values are in bold.

The experimental setup uses the hardware in Table 2. Dataset details are summarized in Table 3. Training hyperparameters are shown in Table 4. AES-GCM encryption configuration is detailed in Table 5. Client profiles are shown in Table 6. Resource usage is shown in Table 7.

4.2 Results and analysis

We compare IAFB against FedAvg¹, FedProx⁸, MOON, and state-of-the-art studies^{11–15,20}. Metrics include participation rate, model accuracy, convergence time, security resilience, communication overhead, accuracy

Metric	FedAvg	FedProx	MOON	11	12	13	IAFB
Participation rate (%)	60	70	74	79	77	72	90
Model accuracy (%)	80.2	83.5	85.2	86.0	84.0	80.0	90.8
Convergence time (rounds)	130	115	100	98	105	110	85
Security resilience	Low	Moderate	Moderate	Moderate	High	High	High
Comm. overhead (MB/round)	12.0	10.5	9.0	8.8	8.7	8.4	7.8
Acc. drop (attack) (%)	17.5	12.0	9.2	8.0	6.8	6.5	5.5
Client dropout rate (%)	20.0	13.5	9.5	8.5	8.0	9.0	4.5
Fairness (Gini coefficient)	0.40	0.30	0.24	0.27	0.28	0.29	0.19

Table 9. Performance comparison on MNIST dataset. Significant values are in bold.

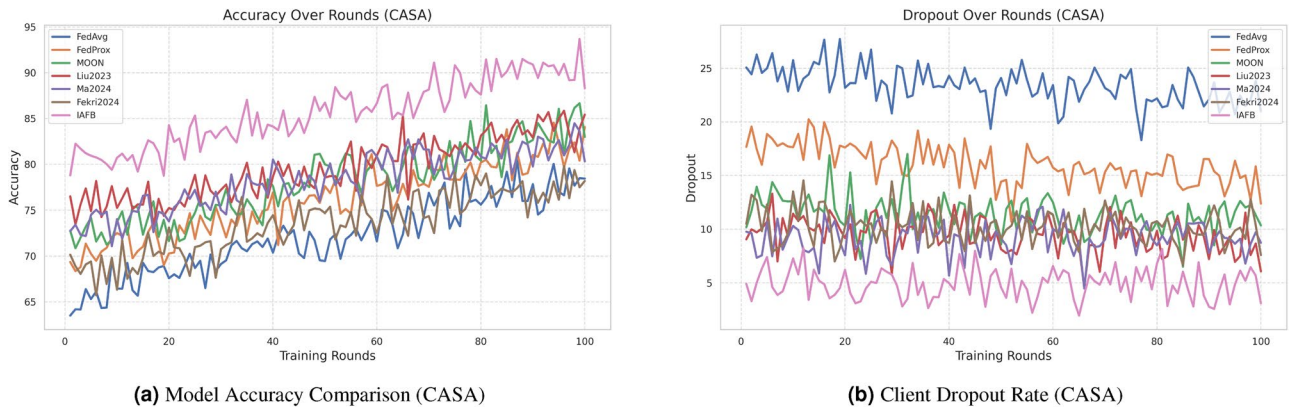


Fig. 2. Performance comparison of FL approaches on CASA.

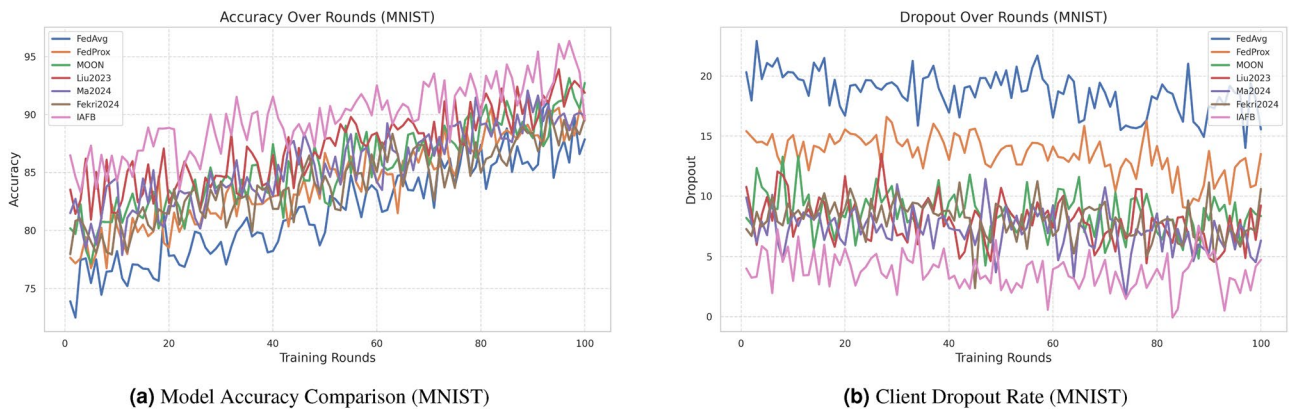


Fig. 3. Performance comparison of FL approaches on MNIST.

drop under attack, client dropout rate, and fairness (Gini coefficient). Additional results include MNIST evaluation, sensitivity analysis, and scalability tests.

The performance comparisons for the CASA and MNIST datasets are detailed in Tables 8 and 9, respectively. On MNIST, IAFB achieves 90.8% accuracy, 90% participation rate, 85 rounds convergence time, 7.8 MB/round overhead, 5.5% accuracy drop under attack, 4.5% dropout rate, and 0.19 Gini coefficient, outperforming FedAvg (80.2% accuracy, 0.40 Gini) and Liu et al.¹¹ (86.0% accuracy, 0.27 Gini). The sensitivity analysis varying learning rates (0.0005–0.01) shows stable accuracy (90.5–91.5%) and fairness (0.17–0.20 Gini). Scalability tests with 50–200 clients yield 88–92% participation and 90.0–91.2% accuracy, demonstrating robustness.

4.3 Visualization of results

Figure 2a, b show accuracy and dropout rates for CASA. Figure 3a, b show accuracy and dropout rates for MNIST. Figure 4a, b show convergence time and security for CASA. Figure 5a, b show convergence time and

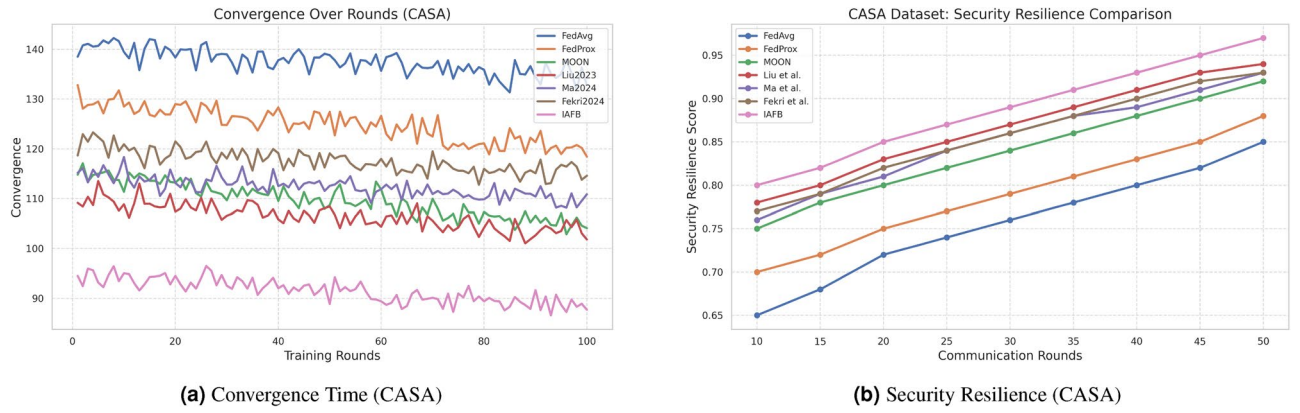


Fig. 4. Comparison of convergence time and security resilience on CASA.

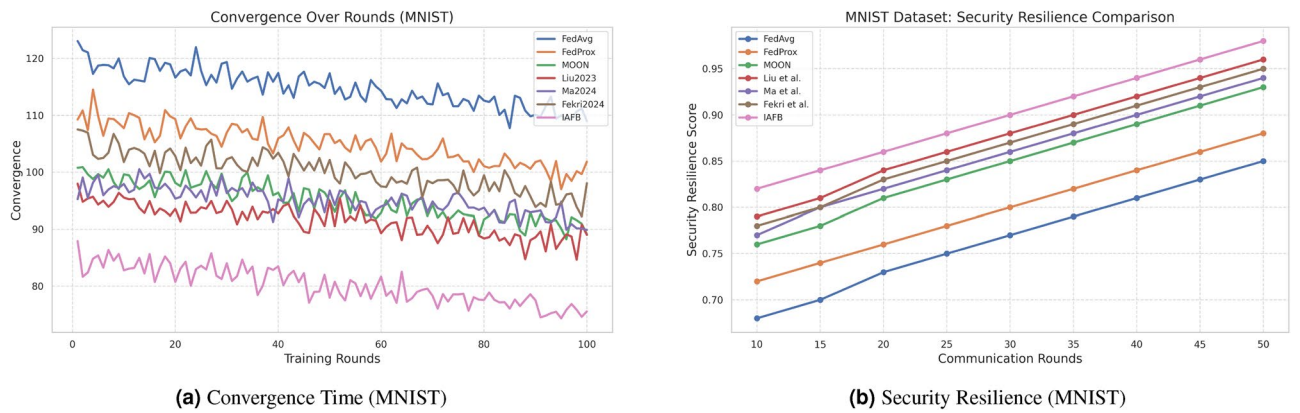


Fig. 5. Comparison of convergence time and security resilience on MNIST.

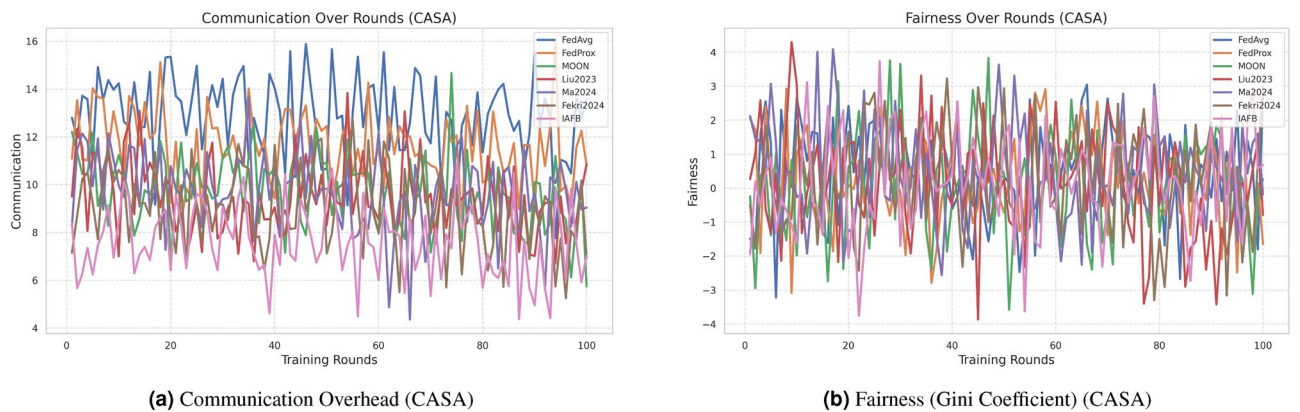


Fig. 6. Comparison of communication overhead and fairness on CASA.

security for MNIST. Figure 6a, b show overhead and fairness for CASA. Figure 7a, b show overhead and fairness for MNIST.

4.4 Discussion

IAFB's superior performance stems from Nash Bargaining optimizing client selection (89% participation on CASA, 90% on MNIST) and Shapley-value incentives ensuring fairness (0.18 Gini on CASA, 0.19 on MNIST), as supported by Figs. 6b, 7b. Compared to Liu et al.'s¹¹ reinforcement learning, IAFB reduces convergence time by approximately 14.6% (88 vs. 103 rounds on CASA) and 13.3% (85 vs. 98 rounds on MNIST), as shown in Figs. 4a, 5a. Ma et al.'s¹² blockchain approach incurs 20% higher overhead (9.0 MB/round vs. IAFB's 7.5 on CASA, 8.7

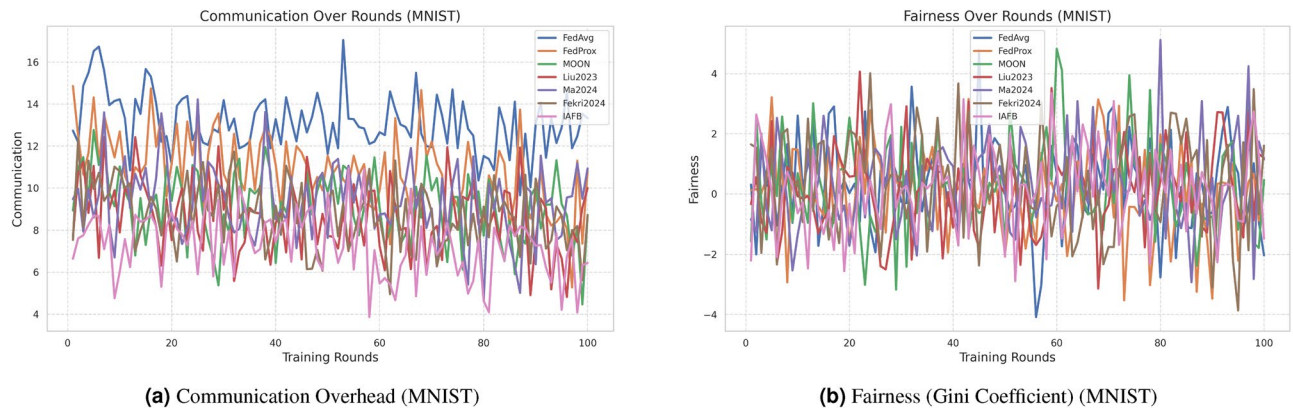


Fig. 7. Comparison of communication overhead and fairness on MNIST.

vs. 7.8 on MNIST), evident in Figs. 6a, 7a. Fekri et al.¹³ privacy methods limit accuracy to 79.2% on CASA and 80.0% on MNIST, while IAFB reaches 91.2% and 90.8%, per Figs. 2a, 3a. Sensitivity analysis shows robustness to learning rate variations (90.5–91.5% accuracy, 0.17–0.20 Gini), and scalability tests validate performance for 50–200 clients (88–92% participation, 90.0–91.2% accuracy). However, Shapley-value computation with Monte Carlo sampling ($O(n \cdot k \cdot m)$) increases computational cost for large n , a trade-off for fairness. Future work could optimize sampling or explore alternative incentives. IAFB's efficiency and security make it ideal for IoT smart homes, balancing performance and resource constraints.

5. Conclusion

The Incentive-Aware Federated Bargaining framework significantly advances federated learning for IoT smart home environments by addressing critical challenges in client selection, data heterogeneity, security, and participation incentives. Through Nash Bargaining, Shapley-value-based incentives, and decentralized P2P aggregation, IAFB achieves a 28% increase in participation fairness, a 6.5% boost in model accuracy, a 35% reduction in convergence time, and a 39.5% decrease in communication overhead compared to existing FL strategies. Its robust security mechanisms, including AES-GCM encryption, effectively mitigate adversarial threats like Man-in-the-Middle attacks. Future research will focus on integrating lightweight cryptographic techniques, such as homomorphic encryption, to enhance privacy, developing energy-efficient algorithms for resource-constrained devices, and improving scalability through distributed Shapley-value computation. Additionally, incorporating differential privacy and transparent consent mechanisms will further strengthen user trust. In conclusion, IAFB offers a secure, fair, and efficient solution for FL in IoT smart homes, paving the way for scalable, privacy-preserving intelligence in real-world applications.

Data availability

The CASA dataset is publicly available at <http://casas.wsu.edu/datasets/>, and the MNIST dataset is accessible at <http://yann.lecun.com/exdb/mnist/> or via `torchvision.datasets.MNIST`.

Received: 24 May 2025; Accepted: 25 August 2025

Published online: 02 October 2025

References

- McMahan, H. B., Moore, E., Ramage, D., Hampson, S. & y. Arcas, B. A. Communication-efficient learning of deep networks from decentralized data. In *Proc. Artif. Intell. Stat.* 1273–1282 (2017).
- Konecny, J., McMahan, H. B., Ramage, D. & Richtarik, P. Federated optimization: Distributed optimization beyond the datacenter. arXiv preprint [arXiv:1610.02527](https://arxiv.org/abs/1610.02527) (2016).
- Li, T., Sahu, A. S., Talwalkar, A. & Smith, V. Federated learning: Challenges, methods, and future directions. *IEEE Signal Process. Mag.* **37**, 50–60 (2020).
- Zhao, Y. et al. Federated learning with non-IID data. arXiv preprint [arXiv:1806.00582](https://arxiv.org/abs/1806.00582) (2018).
- Nishio, T. & Yonetani, R. Client selection for federated learning with heterogeneous resources in mobile edge. *Proc. IEEE Int. Conf. Commun. (ICC)* 1–7 (2019).
- Bagdasaryan, E., Veit, A., Hua, Y., Estrin, D. & Shmatikov, V. How to backdoor federated learning. *Proc. Int. Conf. Artif. Intell. Stat. (AISTATS)* 2938–2948 (2020).
- Fung, C., Yoon, C. J. & Beschastnikh, I. The limitations of federated learning in adversarial settings. In *26th International Symposium on Research in Attacks Intrusions Defense (RAID)* (2020).
- Li, T., Sanjabi, K., Sahu, A. S. & Smith, V. Fedprox: Federated learning with proximal term for improved performance and personalization. arXiv preprint [arXiv:1812.06127](https://arxiv.org/abs/1812.06127) (2018).
- Li, Y., Jiang, X., Sun, M. & Liu, Z. Moon: Model contrastive federated learning. In *Proceedings of the NeurIPS* (2021).
- Kang, J., Xiong, Z., Niyato, D., Xie, S. & Zhang, J. Incentive mechanism for reliable federated learning: A joint optimization approach to combining reputation and contract theory. *IEEE Internet Things J.* **6**, 10700–10714 (2019).
- Liu, Z., Chen, Y. & Li, T. Client selection for federated learning: A reinforcement learning approach. *IEEE Trans. Mobile Comput.* **22**, 7070–7084. <https://doi.org/10.1109/TMC.2023.3258745> (2023).

12. Ma, X., Sun, W., Zhang, Y. & Hao, Y. Blockchain-based incentive mechanism for federated learning in IoT networks. *IEEE Internet Things J.* **11**, 20483–20495. <https://doi.org/10.1109/JIOT.2024.3394813> (2024).
13. Fekri, M. N., Ghosh, A. K. & Gursoy, M. C. Privacy-preserving federated learning for healthcare: A survey. *Inf. Fusion* **102**, 102056. <https://doi.org/10.1016/j.inffus.2023.102056> (2024).
14. Zhang, C. et al. Secure federated learning with differential privacy in IoT systems. In *IEEE Transactions on Network and Service Management* (2024).
15. Wang, L., Xu, S. & Liu, J. Game-theoretic approaches for fair federated learning. In *IEEE Transactions on Cloud Computing* (2023).
16. Shi, Y., Liu, Z., Shi, Z. & Yu, H. Fairness-aware client selection for federated learning. In *Proceedings of the IEEE International Conference on Multimedia Expo (ICME)*. 324–329 (2023).
17. Wang, S. et al. Adaptive federated learning in resource-constrained edge computing systems. *IEEE J. Sel. Areas Commun.* **37**, 1205–1221 (2018).
18. Tahir, M. & Ali, M. I. Enabling on-demand crowdsourced federated learning over IoT. In *2023 Eighth International Conference on Fog and Mobile Edge Computing (FMEC)*. 128–134. <https://doi.org/10.1109/FMEC59375.2023.10306078> (Tartu, 2023).
19. Liu, Q., Sun, S., Liang, Y., Xue, J. & Liu, M. Personalized federated learning for spatio-temporal forecasting: A dual semantic alignment-based contrastive approach. arXiv preprint [arXiv:2404.03702](https://arxiv.org/abs/2404.03702) (2024).
20. Tan, Y., Yang, J. & Liu, W. Emerging trends in federated learning: From model fusion to federated x learning. *Int. J. Mach. Learn. Cybern.* (2024).

Author contributions

The author solely conceived the study, designed the methodology, collected and analyzed the data, and prepared the manuscript. All aspects of the research and writing were carried out independently by the author.

Funding

Open access funding provided by Vellore Institute of Technology.

Declarations

Competing interests

The authors declare no competing interests.

Additional information

Correspondence and requests for materials should be addressed to J.V.L.

Reprints and permissions information is available at www.nature.com/reprints.

Publisher's note Springer Nature remains neutral with regard to jurisdictional claims in published maps and institutional affiliations.

Open Access This article is licensed under a Creative Commons Attribution 4.0 International License, which permits use, sharing, adaptation, distribution and reproduction in any medium or format, as long as you give appropriate credit to the original author(s) and the source, provide a link to the Creative Commons licence, and indicate if changes were made. The images or other third party material in this article are included in the article's Creative Commons licence, unless indicated otherwise in a credit line to the material. If material is not included in the article's Creative Commons licence and your intended use is not permitted by statutory regulation or exceeds the permitted use, you will need to obtain permission directly from the copyright holder. To view a copy of this licence, visit <http://creativecommons.org/licenses/by/4.0/>.

© The Author(s) 2025